


RESEARCH ARTICLE

Clusters of Monoisotopic Elements for Calibration in (TOF) Mass Spectrometry

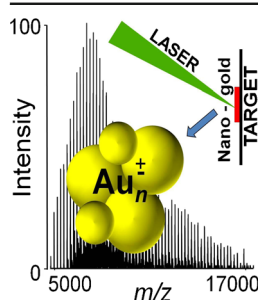
Lenka Kolářová,¹ Lubomír Prokeš,¹ Lukáš Kučera,^{2,3} Aleš Hampl,^{2,3} Eladia Peña-Méndez,⁴ Petr Vaňhara,^{2,3} Josef Havel^{1,3} 

¹Department of Chemistry, Faculty of Science, Masaryk University, Kamenice 5/A14, 625 00, Brno, Czech Republic

²Department of Histology and Embryology, Faculty of Medicine, Masaryk University, Brno, Czech Republic

³International Clinical Research Center, St. Anne's University Hospital, Pekařská 53, 656 91, Brno, Czech Republic

⁴Departamento de Química, Unidad Departamental de Química Analítica, Facultad de Ciencias, Universidad de La Laguna (ULL), Avda. Astrofísico Fco. Sánchez, s/n, 38206, La Laguna, Spain



Abstract. Precise calibration in TOF MS requires suitable and reliable standards, which are not always available for high masses. We evaluated inorganic clusters of the monoisotopic elements gold and phosphorus ($\text{Au}_n^+/\text{Au}_n^-$ and $\text{P}_n^+/\text{P}_n^-$) as an alternative to peptides or proteins for the external and internal calibration of mass spectra in various experimental and instrumental scenarios. Monoisotopic gold or phosphorus clusters can be easily generated in situ from suitable precursors by laser desorption/ionization (LDI) or matrix-assisted laser desorption/ionization mass spectrometry (MALDI-MS). Their use offers numerous advantages, including simplicity of preparation, biological inertness, and exact mass determination even at lower mass resolution. We used citrate-stabilized gold nanoparticles to generate gold calibration

clusters, and red phosphorus powder to generate phosphorus clusters. Both elements can be added to samples to perform internal calibration up to mass-to-charge (m/z) 10–15,000 without significantly interfering with the analyte. We demonstrated the use of the gold and phosphorous clusters in the MS analysis of complex biological samples, including microbial standards and total extracts of mouse embryonic fibroblasts. We believe that clusters of monoisotopic elements could be used as generally applicable calibrants for complex biological samples.

Keywords: Monoisotopic elements, Calibration, Gold clusters, Phosphorus clusters, TOF mass spectrometry

Received: 5 October 2016/Revised: 22 November 2016/Accepted: 25 November 2016/Published Online: 19 December 2016

Introduction

Calibration is a crucial step in almost all instrumental analytical methods. Calibration in time-of-flight mass spectrometry (TOF MS) is mostly based on calibration standards, such as commercially available mixtures of purified peptides and proteins of known masses; polymeric standards, like polyethylene glycol, polypropylene glycol, and polyalanine [1]; or synthetic macromolecules, such as polyester dendrimers (SpheriCal) [2]. These common calibration standards require high instrumental resolution to reveal their accurate masses and

can suffer from low stability and differential ionization due to mutual competition during ionization. Moreover, accurate calibration using peptide standards is complicated by the non-Gaussian distribution of ^{13}C isotopes in proteins over m/z 5 kDa [3]. The price of commercially available standards and the accuracy of in-house preparation protocols are also relevant issues. Therefore, there is a need for alternative calibrants with improved parameters.

Carbon clusters are suitable for the calibration of the tandem Penning-trap mass spectrometric system for the high-precision online detection of short-lived isotopes or heavy radionuclides up to a mass of 240 Da [4, 5]. On the other hand, carbon clusters are not suitable for calibration in higher mass ranges because of their complex isotopic envelope.

Monoisotopic elements, such as phosphorus or cesium, and their clusters have already been proposed for the calibration of mass spectra [6–9]. Clusters composed of isotopically pure

Electronic supplementary material The online version of this article (doi:10.1007/s13361-016-1567-x) contains supplementary material, which is available to authorized users.

Correspondence to: Josef Havel; e-mail: havel@chemi.muni.cz

elements that consist of only one stable isotope offer a great advantage. Clusters of monoisotopic elements provide simple spectra with many monoisotopic peaks covering the mass range of interest with regular mass spacing. In this work, we discuss the calibration of mass spectra by clusters of red phosphorus, which is already established in our laboratory [6, 10–16], and compare it with calibration by gold clusters generated directly on the target by laser desorption ionization (LDI)-MS of various materials, including gold foil [17], various types of gold nanoparticles (AuNPs), chloroauric acid (HAuCl_4), a mixture of 2-(4-hydroxyphenylazo) benzoic acid and HAuCl_4 [18], and polyvinylpyrrolidone-stabilized AuNPs [19]. Gold clusters provide simple and fast determination of accurate mass compared with common calibration standards, such as peptides or proteins. Moreover, AuNPs can enhance ionization in various techniques, such as surface-assisted laser desorption ionization (SALDI), nanoparticle-assisted laser desorption ionization (NALDI), and gold nanoparticle-assisted laser desorption ionization (GALDI) [20–22]. The structure and properties of gold and phosphorus clusters are well known [23–26].

Although the possibility of using gold clusters in negative ion mode (up to m/z 10,000) for the calibration of large biomolecules [17] has already been suggested, the experimental application of gold clusters for the calibration of TOF MS or quadrupole ion trap (QIT)-TOF MS has not yet been published.

Stoermer et al. [27] used a polycrystalline gold target to extensively study the use of gold cluster formation and demonstrated the formation of Au_n^+ (n up to 100). Kéki et al. described the generation of positively charged gold clusters up to m/z 18,000 in positive reflectron ion mode, but they identified only single isotopic peaks for clusters with masses up to 3000 Da and reported the presence of hydride-type ions like Au_nH^+ [18]. Furthermore, they did not provide a detailed evaluation and statistical analysis. Recently, we demonstrated that gold clusters generated from flower-like AuNPs can provide a precise internal calibration standard in SALDI analysis of peptides [22]. That work caused us to ask whether gold clusters are suitable for precise mass determination and the subsequent calibration of TOF analyzers.

In this paper, we provide a comprehensive comparative study of the use of monoisotopic clusters derived from either red phosphorus or gold nanoparticles generated from citrate-stabilized flower-like AuNPs in both positive and negative linear and reflectron ion modes for the external and internal calibration of TOF and QIT-TOF MS.

Experimental

Chemicals

Auric acid (HAuCl_4), α -cyano-4-hydroxycinnamic acid (CHCA), trifluoroacetic acid (TFA), angiotensin I and II, triammonium citrate, and ethanol were purchased from Sigma-Aldrich (Steinheim, Germany). Acetonitrile (ACN; purity for isotachopheresis) and triethanolamine were purchased from Merck (Darmstadt, Germany). Red phosphorus was

purchased from Riedel de Haën (Hannover, Germany). Ethylene glycol was purchased from Lachema (Neratovice, Czech Republic). Citric acid was purchased from PENTA (Chrudim, Czech Republic). Water was double distilled using a quartz apparatus from Heraeus Quarzschmelze (Hanau, Germany). All other reagents were analytical grade. IVD bacterial test standard (BTS) was purchased from Bruker Daltonik GmbH (Bremen, Germany).

Gold Nanoparticles and Sample Preparation for MS

Flower-like and polyhedral AuNPs were synthesized according to procedures described elsewhere [28, 29]. Sample preparation and reaction conditions were described in previous work [22]. Both flower-like and polyhedral AuNPs were collected by centrifugation at 16,000 g for 15 min at 21 °C, washed several times with water, and resuspended at the desired concentration (1.6 mM for flower-like AuNPs and 0.24 mM for polyhedral AuNPs) in double-distilled water. For LDI-MS of the AuNPs, a mixture containing 0.5 mL AuNPs and 0.5 mL citrate aqueous solution (37.5 mM triammonium citrate/25 mM citric acid) was prepared. One microliter of the solution was then deposited on the sample plate and dried at room temperature. For the internal calibration of BTS, 1 μL AuNPs was spotted over the dried drop of BTS prepared according to the Bruker Daltonics GmbH protocol. For the internal calibration of angiotensin I and II, 1 μL peptide mixture was spotted onto the target and allowed to dry; 1 μL 5 mg/mL CHCA matrix (solution for matrix: 50% ACN, 1% TFA) was then spotted onto the target and allowed to dry; and 1 μL red phosphorus (10 mg/mL) was then spotted onto the target. The final concentrations of angiotensin I and II on the target were 4 μM and 6 μM , respectively. The amounts of angiotensin I and II were 4 pmol and 6 pmol per spot, respectively, resulting in 0.7 pmol/ mm^2 and 1 pmol/ mm^2 , respectively.

Cell Culture and Cell Sample Preparation

Mouse embryonic fibroblasts (MEFs) derived from the CF1 mouse strain were cultured at 37 °C in a humidified atmosphere containing 5% CO_2 on tissue culture dishes coated with 0.1% gelatin from Sigma-Aldrich (Prague, Czech Republic) in knockout Dulbecco's modified Eagle's medium (Invitrogen Life Technologies, Prague, Czech Republic) supplemented with 10% fetal bovine serum, 2 mM L-glutamine, 1% minimum essential medium non-essential amino acids, and 1% penicillin-streptomycin, all from Invitrogen/Gibco Life Technologies. The MEFs were harvested by TryPLE Express (1 \times) for 2 min at 37 °C, washed in 1 \times phosphate buffered saline, and counted. To eliminate traces of phosphate buffered saline, the cells were centrifuged (relative centrifugal force 100 g , 2 min) and washed three times in 1 mL 150 mM ammonium bicarbonate buffer. MEF extracts were prepared by osmotic lysis of 1×10^6 cells in 1 mL water. The MEF extracts were then mixed at a 1:1 ratio with matrix containing 10 mg/mL CHCA in 70% ACN, 29% water, and 1% TFA; then 0.5 μL of the mixture was then spotted onto the target plate.

Acquisition of Mass Spectra

Mass spectra were recorded using either an AXIMA CFR TOF mass spectrometer or an AXIMA Resonance QIT-TOF mass spectrometer, both from Kratos Analytical Ltd. (Manchester, UK). Brief schematics of the devices are given in Supplementary Scheme S1 (On-line Resource 3). Both devices were equipped with a microchannel plate detector and used a nitrogen laser (337 nm) and delayed extraction. The laser energy was expressed in arbitrary units (a.u.) ranging from 0 to 180 a.u. The laser power and fluence at 180 a.u. were 6 mW and ≈ 10 mJ/mm²/pulse, respectively. The accelerating voltage was set to 20 kV for all of the measurements. All experiments were performed in repetition mode at a frequency of 5 Hz and with a pulse time width of 3 ns. The diameter of the irradiated spot was approximately 150 μ m. Analyses were carried out at 10^{-4} Pa pressure in the TOF tube, and each mass spectrum was recorded by accumulating the spectra from at least 500 laser shots. All measurements were performed in positive and/or negative linear and/or reflectron ion modes. AXIMA Resonance operates solely in positive/negative reflectron ion mode. Therefore, the AXIMA CFR instrument was used for all linear measurements. The AXIMA Resonance instrument was equipped with a QIT mass analyzer. Mass spectra were recorded in the following ranges: m/z 100–400, 250–1200, 800–3500, 1500–8000, and 3000–15,000. The pressure in the ion source was typically 6×10^{-6} Torr. Spatial focusing was provided by two Einzel lenses separated by a pyramid mirror, and ions were injected axially into the trap. During ion introduction, no rf potential was applied to the ion trap. To trap ions, a retarding potential was applied to the end cap adjacent to the time-of-flight, and an rf with a frequency of 500 kHz was applied to the ring electrode (rapid rf-startup). Amplitudes and corresponding bias voltages were chosen according to the analyte mass under investigation. The rapid rf-startup method provides a trapping efficiency close to 100%. Once trapped, the ions were cooled using argon. The pressure in the trap was held at 6×10^{-3} Torr. QIT has two functions: trapping externally generated MALDI ions and providing a collision cell for MS/MS experiments. All mass spectra were recorded automatically using a regular raster. Mass spectra were plotted as the ion signal relative to the m/z value. The ion signal was defined as the current induced by the impact of the ions on the microchannel plate detector expressed in mV. The spectra were normalized so that the intensity of the maximum peak = 100%. The sample plate was a 2-mm thick stainless steel plate containing 384 wells with a sample spot diameter of 2.8 mm (area = 6 mm²). To avoid carryover contamination, the target plate was regularly cleaned with 96% ethanol and double-distilled water in an ultrasonic bath and dried before the samples were spotted. The Launchpad software (Kompact ver. 2.3.4, 2003) from Kratos Analytical Ltd. was used to evaluate the mass spectra in all experiments.

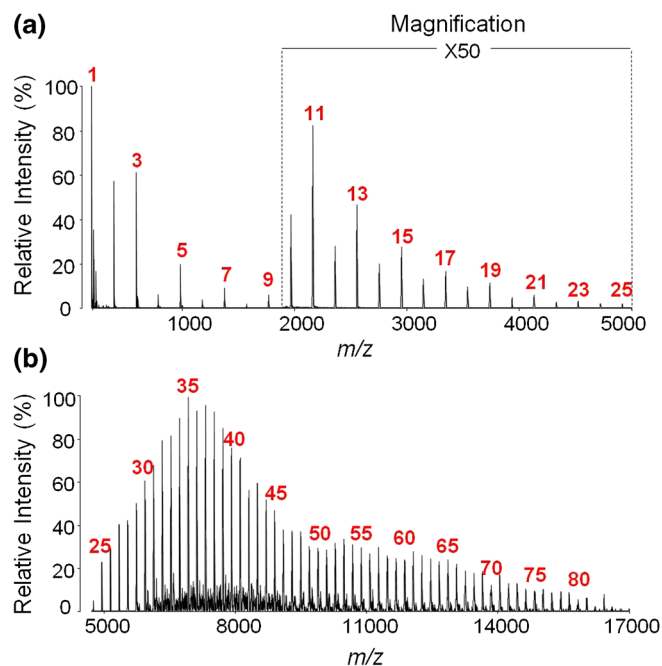


Figure 1. Mass spectra of gold clusters generated by LDI of citrate-stabilized flower-like AuNPs in positive linear ion mode by AXIMA CFR MALDI-TOF MS. **(a)** Spectrum in low mass range m/z 190–5000, and **(b)** higher mass range m/z 5000–17,000. Conditions: average of 500 laser shots, 120 and 170 a.u. laser energy, 100% intensity corresponds to **(a)** 256 mV, and **(b)** 66 mV. Selected n values of Au_n^+ clusters are given in red

Results and Discussion

Precise instrumental calibration is a limiting step in mass spectrometry of biomolecules, especially that of complex biological samples such as peptide and protein mixtures or cell extracts. We performed a comprehensive study of the use of inorganic, monoisotopic gold clusters for the calibration of biomolecules including peptides, bacterial extracts, and total extracts of eukaryotic cells.

Gold Clusters ($Au_n^{+/-}$)

We generated gold clusters ($Au_n^{+/-}$) from citrate-stabilized, flower-like AuNPs in positive and negative linear ion modes. Clusters generated from flower-like AuNPs provide LDI spectra with a slightly wider mass range of Au peaks than those provided by clusters generated from polyhedral AuNPs.

Table 1. Mass Accuracy of $Au_n^{+/-}$ Cluster Peaks Determination

		m/z range		
		100–2000	2000–5000	7000–14,000
Ion modes	Lin +	47 ppm	19 ppm	26 ppm
	Lin -	48 ppm	-	-
	Ref +	4 ppm	4 ppm	-
	Ref -	5 ppm	4 ppm	-

- No peaks or intensities of $Au_n^{+/-}$ clusters too low for detection

Effective ionization of higher gold clusters began at a laser energy of 120 a.u., and gradual increase of the laser energy resulted in the generation of higher gold clusters in both positive and negative linear ion modes (Figure 1). In positive and negative linear ion modes at maximum laser energy, we achieved Au clusters up to m/z 17,000 and m/z 6000, respectively. In positive and negative reflectron ion modes at maximum laser energy, we achieved Au clusters up to m/z 7000 and m/z 6000, respectively. The LDI at higher laser energies of flower-like AuNPs without citrate buffer led to decomposition of the gold clusters (data not shown).

Representative LDI mass spectra of citrate-stabilized flower-like AuNPs in positive ion mode are shown in Figure 1. We observed Au_n^+ clusters ranging in size from $n=1$ up to $n=25$ in the mass range m/z 180–5000 (Figure 1a). We detected additional peaks of clusters of $AuNH_3^+$, $Au(NH_3)_2^+$, and $Au_3NH_3^+$ with very low intensity in the spectrum, probably from the citrate buffer. We observed Au_n^+ clusters ranging in size from $n=25$ up to $n=80$ in the mass range m/z 5000–17,000 (Figure 1b). We observed additional small peaks at cluster sizes of $n=30$ or greater, the nature of which was

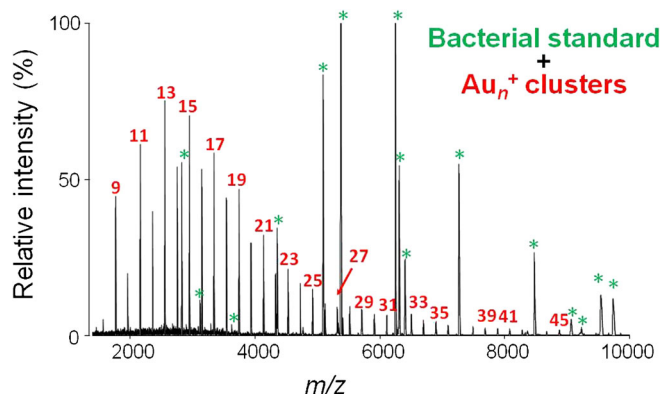


Figure 3. Spectrum of gold clusters (Au_n^+ , red numbers) with peptides/proteins (green stars) from bacterial test standard. Conditions: linear positive mode, 135 a.u. laser energy, mass range m/z 1400–10000, 100% intensity corresponds to 11 mV

unclear. We speculate that NH_4^+ -Au or Au-Fe can form during high laser energy impacts.

We evaluated calibration in three mass ranges: low (m/z 180–2100), medium (m/z 2000–7000), and high (m/z 7000–

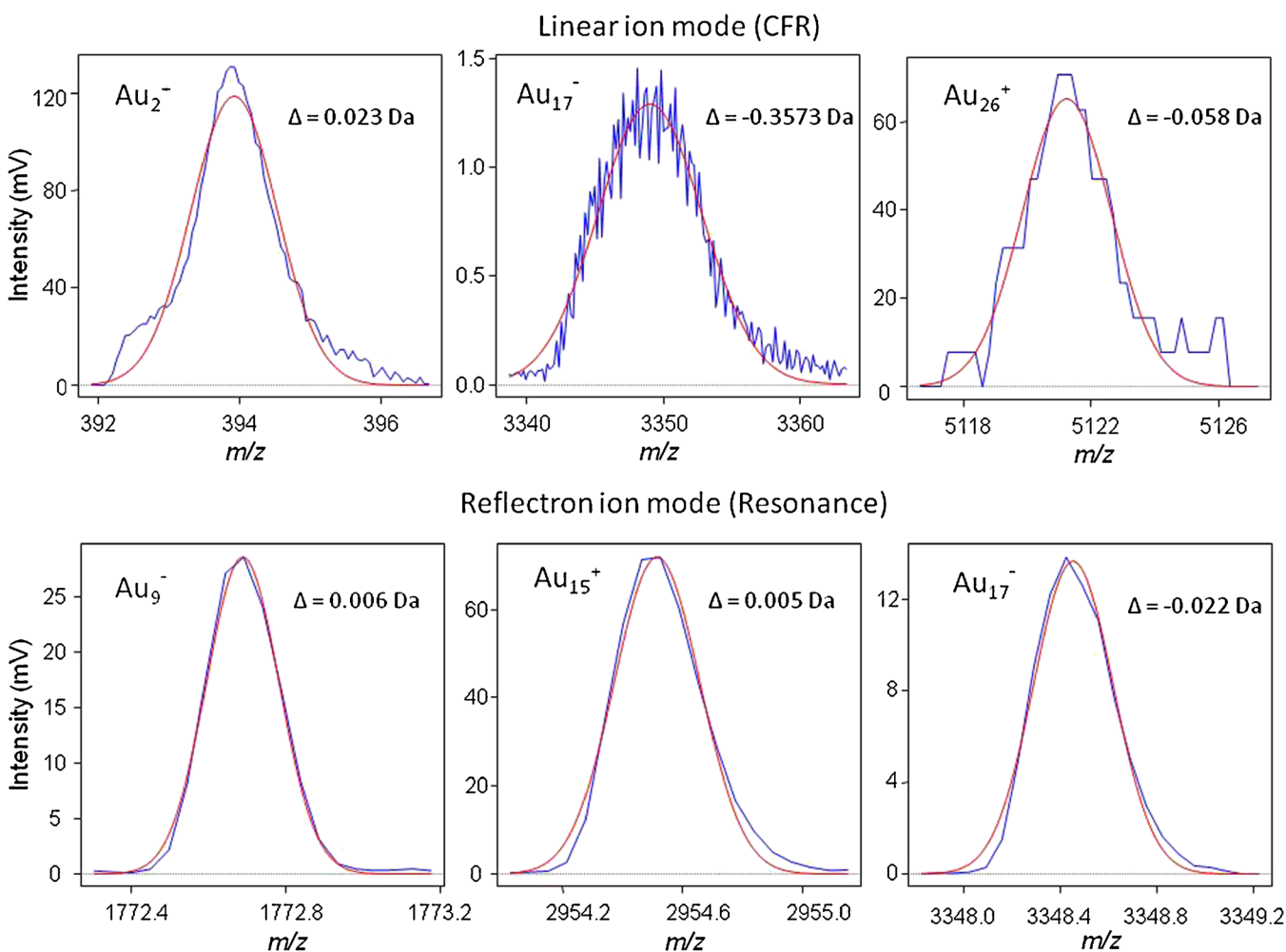


Figure 2. Statistical evaluation of the shape of Au_n cluster peaks fitted to a Gaussian curve (smooth line in red is a Gaussian curve, $\Delta = (m/z)_{\text{theoretical}} - (m/z)_{\text{experimental}}$). Details are given in On-line Resource 1; $(m/z)_{\text{theoretical}}$ is the monoisotopic value according to IUPAC. The experimental value is that found using the Gaussian profile of the peak

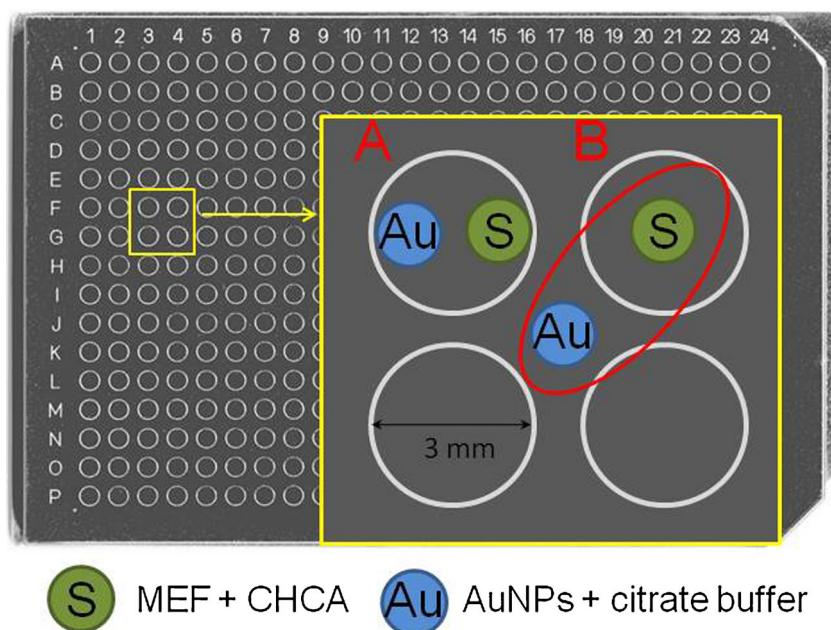


Figure 4. Sample deposition on the steel target plate for semi-internal calibration. Position A: calibrant and sample are spotted to the same well. Position B: calibrant is situated in the center of four neighboring wells. Au = AuNPs; S = sample

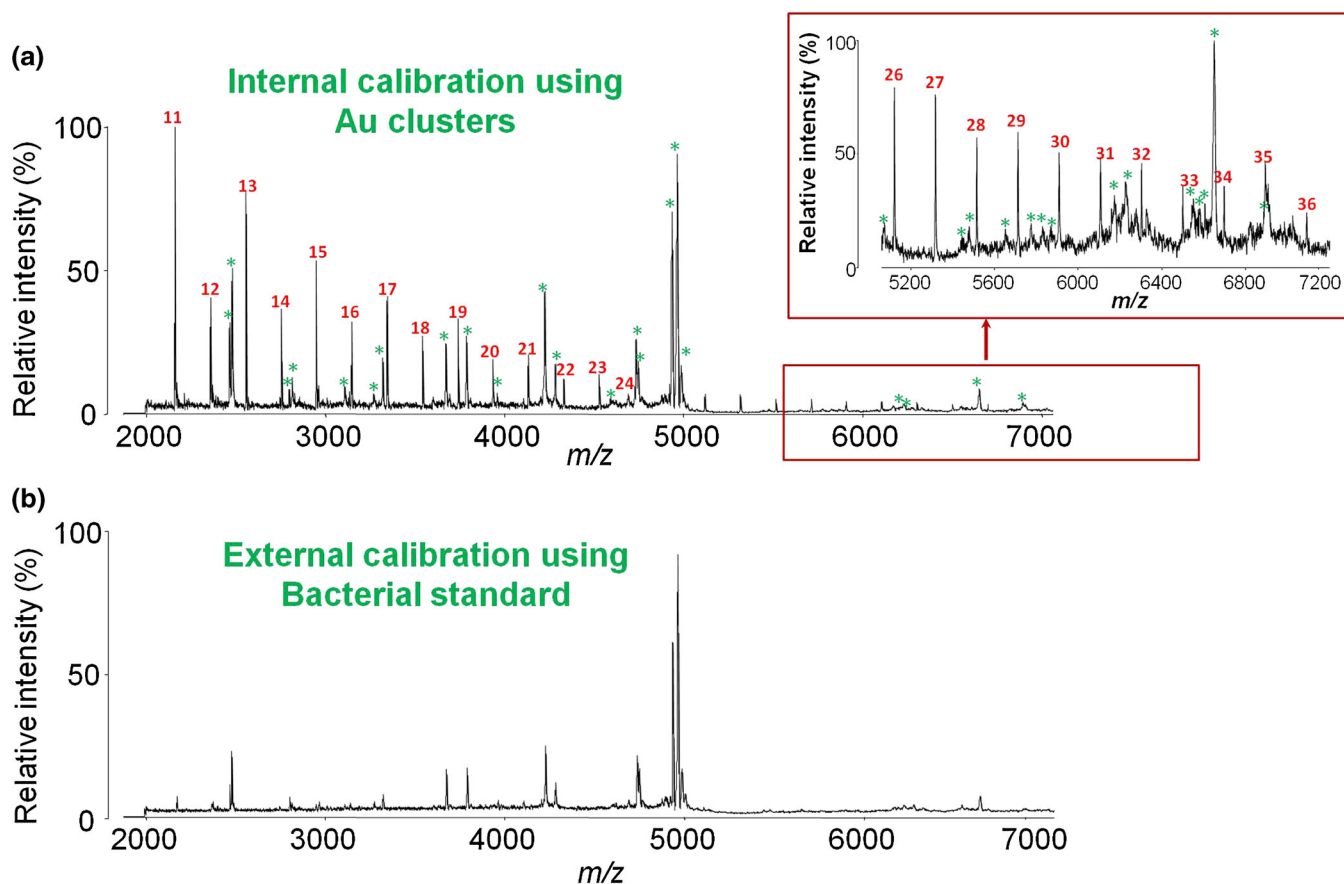


Figure 5. Spectrum of gold clusters (Au_n^+ , red numbers) with peptides/proteins (green stars) from mouse embryonic fibroblasts. Mass spectrum of mouse embryonic fibroblasts with (a) internal calibration using Au_{11-35}^+ clusters with mass accuracy ± 7 ppm, and (b) external calibration using Bacterial Test Standard with mass accuracy ± 33 ppm. Conditions: positive linear ion mode, 95 and 130 a.u. laser energy, mass range m/z 2000–7200, 100% corresponds to (a) 26 mV, and (b) 45 mV

14,000). The intensity of Au clusters from m/z 14,000 up to m/z 17,000 was less than 1 mV and was thus not suitable for calibration. Therefore, we used only the peaks with intensity higher than 1 mV. Peak maxima were determined by Gradient-Centroid peak detection. Table 1 summarizes the accuracy of the mass of the Au clusters in each ion mode, with each value calculated as an average of the absolute errors of mass determination in ppm. The mass list of the gold cluster values (theoretical and experimental), differences between the theoretical and experimental masses, and calculated errors in absolute value of ppm are summarized in Supplementary Tables S1–S8 (On-line Resource 1). The corresponding spectra in the individual modes are shown in Supplementary Figures S1–S8 (On-line Resource 1).

The use of gold clusters for calibration has several advantages. The synthesis of gold nanoflowers or polyhedral AuNPs is facile, fast, and cheap. The determination of the masses of Au clusters is simple and precise because of the mono-isotopicity of gold. Statistical evaluation (Figure 2) of the peak shapes confirmed that the peaks followed an almost perfect Gaussian waveform. Thus, from our results we can conclude that gold clusters are suitable for the calibration of TOF/QIT-TOF analyzers in both low and high mass ranges.

Recently, we showed that flower-like AuNPs deposited on the target plate enhance the ionization of peptides [17]. We were curious whether the gold clusters generated by high-energy LDI could be used for the internal calibration of biomolecules such as small peptides or even proteins. We mixed peptides or BTS with gold flower-like AuNPs and

recorded the mass spectra. The generated gold clusters did not interfere with the peptides or proteins, and the peaks of the clusters were clearly distinguishable among the peaks of the analyte (Figure 3). Based on this promising observation, we investigated whether the same approach could be applied to highly complex mixtures of biomolecules, such as the total extracts of eukaryotic cells. First, we tested the generation of gold clusters from flower-like AuNPs in mixture with total MEF extract. However, the efficacy of fragmentation of the flower-like AuNPs was rather unsatisfactory, and we found virtually no peaks of gold clusters (data not shown). Therefore, we introduced a different calibration approach in which total MEF extract with CHCA matrix and flower-like AuNPs in citrate buffer were spotted separately, either on the sample spot or in close mutual proximity (Figure 4). The samples were close to the calibrant; the distance between them was maximally 1.5 mm. The spotting of the samples is shown in Figure 4. We changed the position of the laser beam and the value of the laser energy manually during the measurement. When the spectra of a sample showed sufficient intensity (from a minimum of 300 laser shots), we moved the position of the laser beam toward that of the calibrant. We increased the laser energy to effectively generate gold clusters and recorded a minimum of 300 profiles of the calibrant. The optimal laser energy for the ionization of the components of the cell extract was 95 a.u., but a minimum laser energy of 130 a.u. was required to effectively generate Au_n^+ clusters. Therefore, we first recorded the signals of the MEF extract at 95 a.u. laser energy. Then, without any interruption of

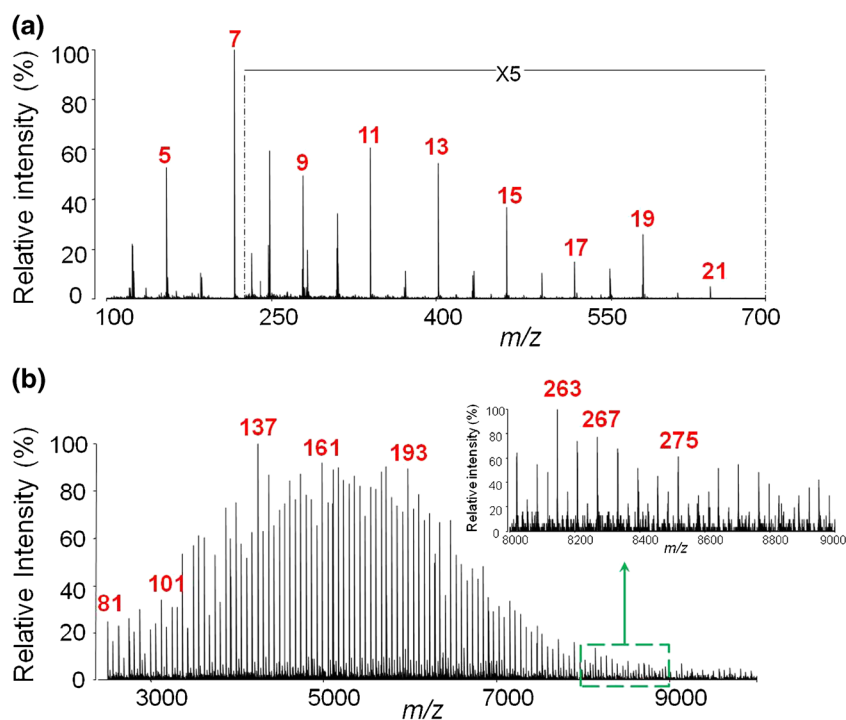


Figure 6. Mass spectrum demonstrating the generation of phosphorus clusters by LDI of red phosphorus in positive reflectron ion mode by AXIMA Resonance MALDI-QIT-TOF MS. (a) Spectrum in low mass range m/z 100–700, and (b) higher mass range m/z 2500–10,000. Conditions: average of 1000 laser shots, 100 and 120 a.u. laser energy, 100% intensity corresponds to (a) 81 mV, and (b) 2 mV. Selected n values of P_n^+ clusters are given (in red)

Table 2. Mass Accuracy of $P_n^{+/-}$ Cluster Peaks Determination

		m/z range		
		100–1000	2000–5000	5000–14,000
Ion modes	Lin +	25 ppm	-	-
	Lin -	194 ppm	-	-
	Ref +	5 ppm	7 ppm	-
	Ref -	8 ppm	4 ppm	-

- No peaks or intensities of $P_n^{+/-}$ clusters too low for detection

measurement, we increased the laser energy to 130 a.u. and recorded the signal of the Au_n cluster peaks. Thus, we recorded the final spectrum at two energetic levels, obtaining the

peaks of the gold clusters as well as peaks of the MEF extract. In this way, we eliminated the mutual suppression of signals between the cell extract and gold clusters. The calibration using the Au_n clusters produced significantly better results than external calibration with BTS (Figure 5). The mass precision of MEF spectra generated with internal calibration using Au_{11-35}^+ clusters reached ± 7 ppm (± 0.03 Da), whereas that generated with external calibration using BTS reached ± 33 ppm (± 0.2 Da). The comparison of the two MEF spectra calibrated externally using BTS and internally using Au_n^+ clusters, respectively, led to the conclusion that the differences between the signals of the MEFs are about ± 0.3 Da on average. The data evaluation is summarized in Supplementary Tables S1 and S2 in On-line Resource 2.

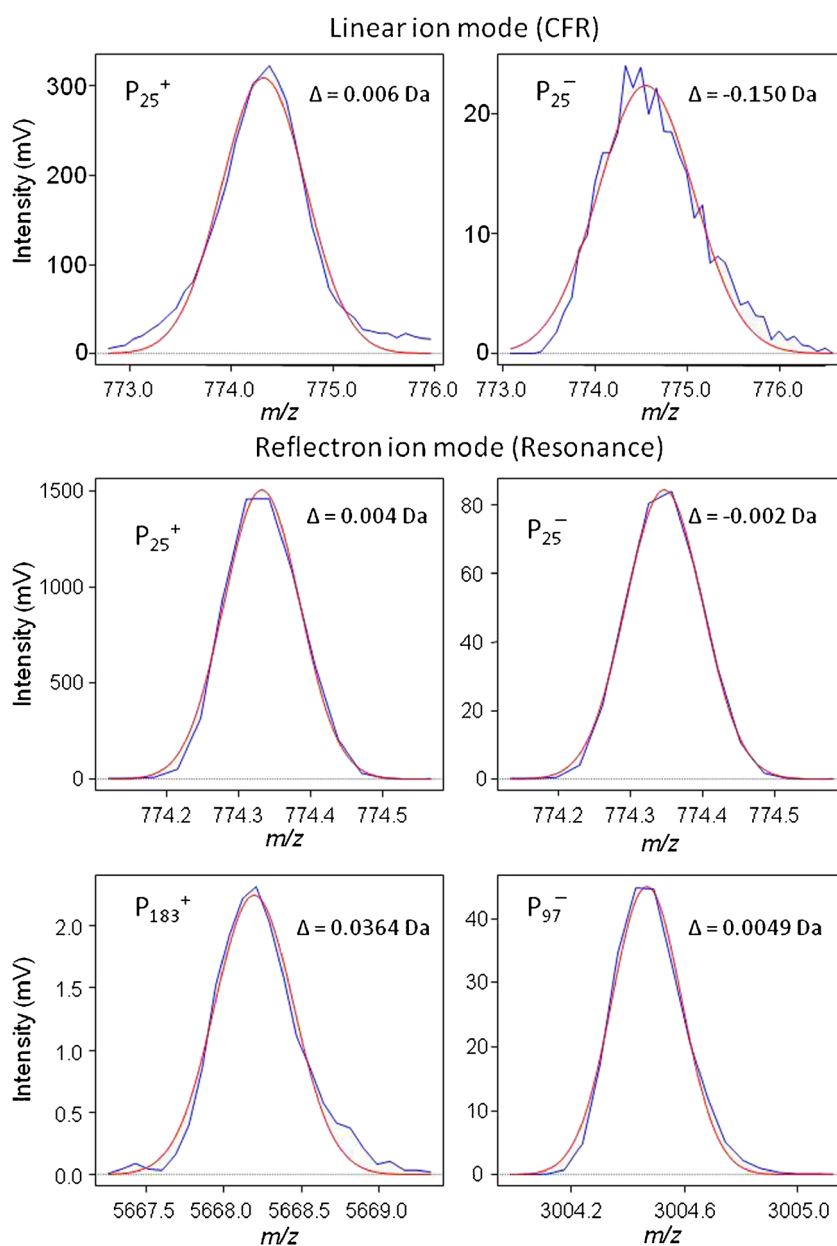


Figure 7. Statistical evaluation of the peak shapes of P_n clusters by the fitting of a Gaussian curve. Smooth line in red is a Gaussian curve, $\Delta = (m/z)_{\text{theoretical}} - (m/z)_{\text{experimental}}$

Overall, our results show that the new calibration approach using gold clusters provides an option for the analysis of highly complex biological samples requiring precise and accurate calibration.

Phosphorus clusters ($P_n^{+/-}$)

Red phosphorus has advantages similar to those of gold. The greatest advantages are its mono-isotopicity and easy formation of peaks of $P_n^{+/-}$ clusters using LDI. In our laboratory, we introduced the calibration of mass spectra using red phosphorus clusters 5 y ago, and we generated excellent results with the technique. The following are new results that extend those of our previous publication [6] regarding of the use of red phosphorus clusters for the calibration of TOF MS in each mode.

We used the AXIMA CFR TOF and AXIMA Resonance QIT-TOF instruments for experiments in linear and reflectron ion modes, respectively. For the generation of $P_n^{+/-}$ cluster peaks, we used a red phosphorus powder. It is recommended that only the peaks of phosphorus clusters with an odd number of phosphorus atoms be used for calibration because peaks with an even number usually have low signal intensity. Moreover, clusters with an even number of peaks may contain hydrogenated forms and therefore entail a high risk of erroneous calibration due to the selection of the wrong peak. At high laser energy in both positive and negative linear ion mode, $P_n^{+/-}$ clusters up to m/z 4000 were achieved. In positive and negative reflectron ion mode at maximum laser energy, we achieved $P_n^{+/-}$ clusters up to m/z 7000 and m/z 10,000, respectively. We achieved higher phosphorus clusters with increased laser energy. We investigated the accuracy of the determination of the phosphorus masses with odd numbers of cluster peaks.

Figure 6 shows selected LDI mass spectra of red phosphorus in positive reflectron ion mode. Figure 6a shows P_n^+ clusters from $n=4$ up to $n=22$ in the mass range m/z 100–700. We detected additional low-intensity peaks of P_4H^+ , P_6H^+ , P_8H^+ , $P_{10}H^+$, $P_{12}H^+$, $P_{14}H^+$, $P_{16}H^+$, and P_7O^+ in the spectrum. Figure 6b shows P_n^+ clusters ($n=81$ up to $n=275$) in the mass range m/z 2500–9000.

We evaluated calibration in three mass ranges: low (m/z 100–1000), medium (m/z 2000–5000), and high (m/z 7000–14,000). The intensity of P_n^+ clusters from m/z 7000–10,000 was less than 1 mV, so those peaks were not suitable for calibration. The mass list of the $P_n^{+/-}$ cluster values (theoretical and experimental), differences between the theoretical and experimental masses, and calculated errors in absolute value of ppm are provided in Supplementary Tables S9–S16 (On-line Resource 1). The corresponding spectra in the individual modes are shown in Supplementary Figures S9–S16 (On-line Resource 1).

For calibration, we used peaks with intensity higher than 1 mV. Table 2 summarizes the accuracy of the mass of the P_n clusters in each ion mode. Peak maxima were determined by gradient-centroid peak detection. Statistical evaluation (Figure 7) of the peak shapes confirmed that the peaks followed an almost perfect Gaussian waveform. From our results, we can conclude that P_n clusters are suitable for the calibration of TOF/QIT-TOF analyzers in both low and high mass ranges.

It is possible to use P_n cluster peaks for the internal calibration of peptides, not only in linear ion mode [6] but also in reflectron ion mode (see Figure 8). One possible disadvantage of internal calibration using P_n cluster peaks is the likelihood of interference with the analyte due to the shorter repetition of the P_n cluster peaks compared with that of Au_n cluster peaks.

In this work, we focused primarily on gold and phosphorus as the prototypical examples of monoisotopic elements. Evidently, clusters of other monoisotopic elements, such as cesium, iodine, or five of lanthanides can be used in similar manner.

Conclusion

We demonstrated that the in situ generation of gold clusters by LDI is suitable for the external and internal calibration of mass spectrometry of biomolecules. The stability, inertness, and monoisotopic nature of gold and phosphorus clusters provide an accurate calibration standard and thus ensure correct mass spectra, even for highly complex biological samples such as peptide mixtures and total cell extracts.

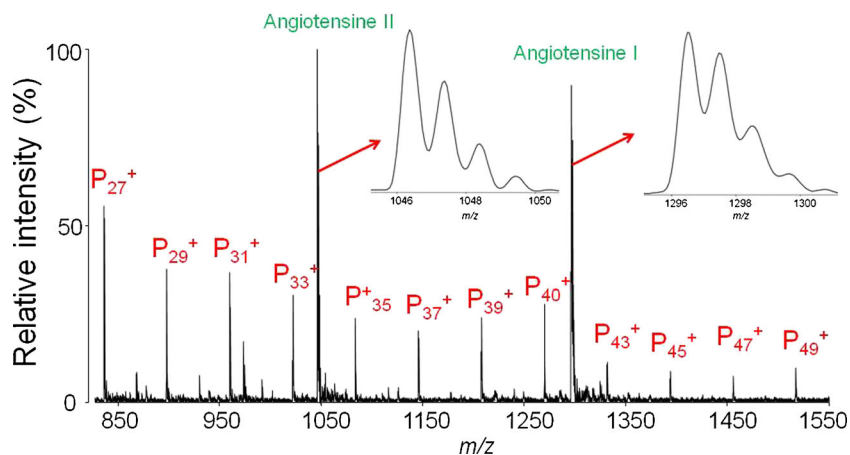


Figure 8. Spectrum of phosphorus clusters (P_n^+ , $n=27-49$) with angiotensin I and II. Conditions: positive reflectron ion mode, 95 a.u. laser energy, mass range m/z 850–1550, 100% intensity corresponds to 495 mV

Acknowledgments

The authors acknowledge support for this work by funds from the National Program of Sustainability II (project no. LQ1605, MEYS CR); Masaryk University, MUNI/A/1352/2015 and Center for Analysis and Modeling of Tissues and Organs (CZ.1.07/2.3.00/20.0185); and the Ministry of Economy and Competitiveness, Spain (MAT2014-57465-R).

References

1. Gruending, T., Sauerland, V., Barahona, C., Herz, C., Nitsch, U.: Polyalanine—a practical polypeptide mass calibration standard for matrix-assisted laser desorption/ionization mass spectrometry and tandem mass spectrometry in positive and negative mode. *Rapid Commun. Mass Spectrom.* **30**, 681–683 (2016)
2. Grayson, S.M., Myers, B.K., Bengtsson, J., Malkoch, M.: Advantages of monodisperse and chemically robust “SpheriCal” polyester dendrimers as a “universal” MS calibrant. *J. Am. Soc. Mass Spectrom.* **25**, 303–309 (2014)
3. Edmondson, R.D., Russell, D.H.: Evaluation of matrix-assisted laser desorption ionization-time-of-flight mass measurement accuracy by using delayed extraction. *J. Am. Soc. Mass Spectrom.* **7**, 995–1001 (1996)
4. Kellerbauer, A., Blaum, K., Bollen, G., Herfurth, F., Kluge, H.-J., Kuckein, M., Sauvan, E., Scheidenberger, C., Schweikhard, L.: Carbon cluster ions for a study of the accuracy of ISOLTRAP. In: Knudsen, H., Andersen, J.U., Kluge, H.-J. (eds.) *Atomic physics at accelerators: stored particles and fundamental physics*, pp. 307–312. Springer, Dordrecht (2003)
5. Chaudhuri, A., Block, M., Eliseev, S., Ferrer, R., Herfurth, F., Martín, A., Marx, G., Mukherjee, M., Rauth, C., Schweikhard, L., Vorobjev, G.: Carbon-cluster mass calibration at SHIPTRAP. *Eur. Phys. J. D.* **45**, 47–53 (2007)
6. Sládková, K., Houška, J., Havel, J.: Laser desorption ionization of red phosphorus clusters and their use for mass calibration in time-of-flight mass spectrometry. *Rapid Commun. Mass Spectrom.* **23**, 3114–3118 (2009)
7. Lou, X., van Dongen, J.L.J., Meijer, E.W.: Generation of CsI cluster ions for mass calibration in matrix-assisted laser desorption/ionization mass spectrometry. *J. Am. Soc. Mass Spectrom.* **21**, 1223–1226 (2010)
8. Mochizuki, S.: Enhanced measurement of CsI cluster ions for mass calibration in MALDI-MS using sugar alcohols. *Anal. Methods* **7**, 2215–2218 (2015)
9. Mochizuki, S.: Effective methods for the measurement of CsI cluster ions using MALDI-MS with suitable solvent combinations and additives. *J. Mass Spectrom.* **49**, 1199–1202 (2014)
10. Pangavhane, S.D., Hebedová, L., Alberti, M., Havel, J.: Laser ablation synthesis of new phosphorus nitride clusters from α -P3N5 via laser desorption ionization and matrix assisted laser desorption ionization time-of-flight mass spectrometry. *Rapid Commun. Mass Spectrom.* **25**, 917–924 (2011)
11. Panyala, N.R., Peña-Méndez, E.M., Havel, J.: Laser ablation synthesis of new gold phosphides using red phosphorus and nanogold as precursors. *Laser desorption ionisation time-of-flight mass spectrometry. Rapid Commun. Mass Spectrom.* **26**, 1100–1108 (2012)
12. Houška, J., Peña-Méndez, E.M., Hernandez-Fernaud, J.R., Salido, E., Hampl, A., Havel, J., Vaňhara, P.: Tissue profiling by nanogold-mediated mass spectrometry and artificial neural networks in the mouse model of human primary hyperoxaluria 1. *J. Appl. Biomed.* **12**, 119–125 (2014)
13. Švihlová, K., Prokeš, L., Skácelová, D., Peña-Méndez, E.M., Havel, J.: Laser ablation synthesis of new gold tellurides using tellurium and nanogold as precursors. *Laser desorption ionisation time-of-flight mass spectrometry. Rapid Commun. Mass Spectrom.* **27**, 1600–1606 (2013)
14. Štěpánová, V., Prokeš, L., Slaviček, P., Alberti, M., Havel, J.: Laser ablation generation of clusters from As-Te mixtures, As-Te glass nanolayers, and from Au-As-Te nanocomposites. *Quadrupole ion trap time-of-flight mass spectrometry. Rapid Commun. Mass Spectrom.* **29**, 1000–1008 (2015)
15. Mawale, R.M., Amato, F., Alberti, M., Havel, J.: Generation of Au(p)Ag(q)Te(r) clusters via laser ablation synthesis using Au-Ag-Te nano-composite as precursor: quadrupole ion-trap time-of-flight mass spectrometry. *Rapid Commun. Mass Spectrom.* **28**, 1601–1608 (2014)
16. Havel, J., Peña-Méndez, E.M., Amato, F., Panyala, N.R., Buršíková, V.: Laser ablation synthesis of new gold carbides. From gold-diamond nanocomposite as a precursor to gold-doped diamonds. *Time-of-flight mass spectrometric study. Rapid Commun. Mass Spectrom.* **28**, 297–304 (2014)
17. Blaum, K., Herlert, A., Huber, G., Kluge, H.-J., Maul, J., Schweikhard, L.: Cluster calibration in mass spectrometry: laser desorption/ionization studies of atomic clusters and an application in precision mass spectrometry. *Anal. Bioanal. Chem.* **377**, 1133–1139 (2003)
18. Kéki, S., Nagy, L., Deák, G., Zsuga, M.: Bimetallic silver-gold clusters by matrix-assisted laser desorption/ionization. *J. Am. Soc. Mass Spectrom.* **15**, 1455–1461 (2004)
19. Tsunoyama, H., Tsukuda, T.: Magic numbers of gold clusters stabilized by PVP. *J. Am. Chem. Soc.* **131**, 18216–18217 (2009)
20. Chen, W.-T., Tomalová, I., Preisler, J., Chang, H.-T.: Analysis of biomolecules through surface-assisted laser desorption/ionization mass spectrometry employing nanomaterials. *J. Chinese Chem. Soc.* **58**, 769–778 (2011)
21. Pilolli, R., Palmisano, F., Cioffi, N.: Gold nanomaterials as a new tool for bioanalytical applications of laser desorption ionization mass spectrometry. *Anal. Bioanal. Chem.* **402**, 601–623 (2012)
22. Kolářová, L., Kučera, L., Vaňhara, P., Hampl, A., Havel, J.: Use of flower-like gold nanoparticles in time-of-flight mass spectrometry. *Rapid Commun. Mass Spectrom.* **29**, 1585–1595 (2015)
23. Häkkinen, H.: Atomic and electronic structure of gold clusters: understanding flakes, cages, and superatoms from simple concepts. *Chem. Soc. Rev.* **37**, 1847–1859 (2008)
24. Zanti, G., Peeters, D.: Electronic structure analysis of small gold clusters Au_m ($m \leq 16$) by density functional theory. *Theor. Chem. Acc.* **132**, 1300 (2012)
25. Pyykkö, P.: Theoretical chemistry of gold. III. *Chem. Soc. Rev.* **37**, 1967 (2008)
26. Bulgakov, A.V., Bobrenok, O.F., Kosyakov, V.I.: Laser ablation synthesis of phosphorus clusters. *Chem. Phys. Lett.* **320**, 19–25 (2000)
27. Stoermer, C., Friedrich, J., Kappes, M.M.: Observation of multiply charged cluster anions upon pulsed UV laser ablation of metal surfaces under high vacuum. *Int. J. Mass Spectrom.* **206**, 63–78 (2001)
28. Jiang, Y., Wu, X.-J., Li, Q., Li, J., Xu, D.: Facile synthesis of gold nanoflowers with high surface-enhanced Raman scattering activity. *Nanotechnology* **22**, 385601–385606 (2011)
29. Wang, W., Chen, Q., Jiang, C., Yang, D., Liu, X., Xu, S.: One-step synthesis of biocompatible gold nanoparticles using gallic acid in the presence of poly-(N-vinyl-2-pyrrolidone). *Colloid. Surf. A Physicochem. Eng. Asp.* **301**, 73–79 (2007)